Substrate potential of last interglacial to Holocene permafrost organic matter for future microbial greenhouse gas production

Janina G. Stapel[1], Georg Schwamborn[2], Lutz Schirrmeister[2], Brian Horsfield[1], Kai Mangelsdorf[1]

[1]GFZ, German Research Centre for Geoscience, Helmholtz Centre Potsdam, Organic Geochemistry, Telegrafenberg, 14473 Potsdam, Germany
[2]Alfred Wegener Institute, Helmholtz Centre for Polar and Marine Research, Department of Periglacial Research, Telegrafenberg, A43, 14473 Potsdam, Germany

Correspondence to: Kai Mangelsdorf (K.Mangelsdorf@gfz-potsdam.de)

Abstract. In this study the organic matter (OM) in several permafrost cores from Bol´shoy Lyakhovsky Island in NE Siberia was investigated. In context of the observed global warming the aim was to evaluate the potential of freeze-locked OM from different depositional ages to act as a substrate provider for microbial production of greenhouse gases from thawing permafrost. To assess this potential, exemplarily the concentrations of free and bound acetate, which form an appropriate substrate for methanogenesis, are determined. The largest free (in pore water) and bound (organic matrix linked) acetate substrate pools are present in layers that cover interstadial MIS 3 and stadial MIS 4 Yedoma permafrost deposits. In contrast, deposits from the last interglacial MIS 5e (Eemian) contain only a small pool of substrates. The Holocene (MIS 1) deposits reveal a significant bound acetate pool, representing a future substrate potential upon release during OM degradation. Additionally, pyrolysis experiments on the OM allocate an increased aliphatic character to the MIS 3 and 4 Late Pleistocene deposits, which might indicate less decomposed and presumably better degradable OM. Biomarkers for past microbial communities including those for methanogenic archaea show also highest abundance during MIS 3 and 4, which indicates that the OM stimulated microbial degradation and presumably greenhouse gas production during time of deposition. On a broader perspective, Arctic warming will increase and deepen permafrost thaw and favour substrate availability from freeze-locked older permafrost deposits. Therefore, especially the Yedoma deposits show a high potential for providing substrates relevant for microbial greenhouse gas production.

1 Introduction

The northern areas of the Eurasian landmass are underlain by permafrost, which is defined as ground that remains under 0 °C for at least 2 consecutive years (Washburn, 1980). These areas represent a large reservoir of organic carbon freeze-locked in the permafrost deposits (French, 2007; Zimov et al., 2009). Hugelius et al. (2014) estimated that about 1300 Pg (1 Pg = 10^{15} = 1 Gt) of soil organic carbon is stored in the upper 0-3 m in the northern circumpolar permafrost regions, which are highly vulnerable to climate warming (Grosse et al., 2011; Schmidt et al., 2011; Mu et al., 2014). Today, Arctic summer temperatures are higher than in the past 400 years (Chapin III et al., 2005). Thus, as a consequence of northern hemisphere

warming an increase in ground temperature, changes in soil drainage, deepening of the active layer (seasonally thawed surface layer), spatial retreat of permafrost and changes in vegetation have already been reported for the Arctic (Davidson and Janssens, 2006; Anisimov, 2007; Romanovsky et al., 2010; Mueller et al., 2015). During permafrost formation low temperatures, anoxic soil conditions and low rates of organic matter (OM) decomposition (Levy-Booth et al., 2007; Schimel and Schaeffer, 2012) resulted in high rates of OM accumulation (Kuhry et al., 2009; Zimov et al., 2009; Schirrmeister et al., 2011a). The currently observed thawing of permafrost promotes the accessibility of accumulated and freeze-locked OM and nutrients for microbial turnover. This results in increased microbial activity and consequently in increased OM decomposition rates (Dutta et al., 2006; Schmidt et al., 2011). Previous studies on permafrost samples from Holocene and Late Pleistocene (LP) Yedoma deposits, which represent widespread ice-rich paleosol formations in NE Siberia, have shown that microbial degradability of the freeze-locked OM seems to depend on the amount and composition of organic carbon rather than on the age of the deposits (Knoblauch et al., 2013; Strauss et al., 2015; Stapel et al., 2016). As observed in incubation experiments on permafrost samples of different ages (Waldrop et al., 2010; Lee et al., 2012; Lipson et al., 2012; Knoblauch et al., 2013; Schadel et al., 2014; Walz et al., 2017), degradation of this OM can lead to enhanced microbial production and release of greenhouse gases such as carbon dioxide and methane to the atmosphere (Wagner et al., 2003; Schuur et al., 2008; McGuire et al., 2009; Knoblauch et al., 2013). This release is expected to have strong feedback on global warming and with that on further permafrost degradation (Schuur et al., 2008). Thus, due to the carbon-climate feedback cycle the permafrost region bears the risk to act as a self-reinforcing system for an increase of global warming.

NE Siberian permafrost formation started already in the Late Pliocene e.g. at today's coasts and islands along the Dmitry Laptev Strait (Arkhangelov et al., 1996). These deposits provide a unique paleo-environmental archive with stratigraphic patterns of long-lasting accumulation periods of permafrost during glacial periods, as well as permafrost degradation features during interglacial periods (Andreev et al., 2004, 2009; Wetterich et al., 2009, 2011). Permafrost deposits were accumulated under continental, cold climate conditions accompanied by syngenetic ice-wedge growth (Wetterich et al., 2011) during glacial periods, e.g. middle Pleistocene (Saalian) and Late Pleistocene (Weichselian; Yedoma deposits) (Andreev et al., 2004; Schirrmeister et al., 2013). In contrast, during the Eemian and the Holocene, extensive thawing of ice wedges and permafrost deposits led to the formation of thermokarst depressions, as well as of thermo-erosional valleys and small rivers (Andreev et al., 2004; Ilyashuk et al., 2006; Wetterich et al., 2009). According to pollen and insect data, the climate of the Eemian resulted in an open grass and grass-sedge tundra similar to the modern situation (Kienast et al., 2008). The mid Eemian environment was characterized by 4-5 °C higher summer temperatures than today with greater seasonal temperature variations in the Northern Hemisphere (Andreev et al., 2004; Dahl-Jensen et al., 2013).

These described environmental changes are expected to have significant impact not only on the amount but also on the composition of the accumulated OM (Strauss et al., 2015; Stapel et al., 2016). After thawing compositional differences in the formerly freeze-locked OM are suggested to have strong effect on the OM biodegradability and with that on the microbial production of greenhouse gases. To obtain deeper insights into the potential of permafrost OM from different ages to act as a substrate provider for intense microbial degradation, we examined characteristic OM parameters and exemplarily low

molecular weight organic acids (LMWOAs) concentrations. LMWOAs such as acetate are important and easily convertible substrates for microbial metabolism (Ganzert et al., 2007). Acetate is a well-known substrate for methanogenesis (Chin and Conrad, 1995). Thus, acetate concentrations provide valuable information on the greenhouse gas production potential of the respective OM (Stapel et al., 2016). Acetate can be dissolved in pore water and cryostructures (e.g. segregated ice) of permafrost deposits. This acetate represents a free substrate pool, which is directly bioavailable for microorganisms. On the other hand acetate can be bound to the organic matrix (e.g. by ester-linkage) forming a future substrate pool upon liberation via geochemical or microbial alteration of the OM (Glombitza et al., 2009; Stapel et al., 2016).

In addition, microbial biomarkers such as phospholipid fatty acids (PLFAs) and glycerol dialkyl glycerol tetraethers (GDGTs) are analysed to examine the interaction between present and past microbial communities with the OM accumulated in the past. Phospholipid esters are essential membrane components of living bacterial cells (Zelles, 1999) and are hydrolysed rapidly after cell death (White et al., 1979; Logemann et al., 2011). Therefore, their fatty acid side chain inventories (PLFAs) are used as an indicator for viable microorganisms in sediments (Haack et al., 1994; Bischoff et al., 2013). In contrast, biomarkers such as GDGTs and archaeol represent membrane lipids of dead microbial biomass, since they are already partly degraded as indicated by the loss of their head groups (Pease et al., 1998). While archaeol and GDGTs with isoprenoid tetraether bridges (isoGDGTs) represent archaeal biomass, GDGTs with branched tetraether bridges (brGDGTs) derive from bacteria (Weijers et al., 2006a and 2006b). However, it should be mentioned that the brGDGTs biomarkers only represent part of the bacterial community (Weijers et al., 2006a and 2006b; Schouten et al., 2013), while the archaeal markers cover most of the past archaeal community (Pancost et al., 2001; Koga and Morii, 2006). In permafrost regions and peatlands archaeol is used as a biomarker for methanogenic archaea (Bischoff et al. 2013; Pancost et al., 2011).

The feedback between climate warming and microbial greenhouse gas generation from thawing permafrost is a topic of large global interest and intensive scientific debate (Zimov et al., 2006; Koven et al., 2011; Schuur et al., 2015). In this context the contribution from thawing OM of different depositional ages to the climate carbon feedback cycle is still unclear. In order to learn more about these interrelations, we conducted a study on Bol´shoy Lyakhovsky Island in the Laptev Sea (NE Siberia). Samples from this region provide the excellent opportunity to investigate permafrost OM deposited from last interglacial to Holocene time. The aims of our study were (1) to assess and compare the stored OM potential for microbial greenhouse gas production in permafrost deposits from different glacial/interglacial periods and (2) to assign this substrate potential to characteristic OM parameters and depositional paleoenvironmental conditions.

2 Study area and material

Bol´shoy Lyakhovsky Island is located between the Laptev and East Siberian seas as the southernmost part of the New Siberian Archipelago (Fig. 1a). During Pleistocene periods of low sea level the island was part of west Beringia, an unglaciated landmass stretching from NE Siberia to Alaska (Hubberten et al., 2004; Andreev et al., 2009). The area is part of the northern tundra zone with an active layer thickness of 30-40 cm and a permafrost thickness of 500-600 m (Andreev et al.,

2004). The study site is located west of the Zimov´e River mouth on the south coast of Bol´shoy Lyakhovsky Island along the Dmitry Laptev Strait (Fig. 1b). The southern coast is characterized by exposed permafrost deposits, while the hinterland is formed by gradually sloping terrain intersected by rivers and valleys developed through thermo-erosion. Based on previous studies the stratigraphy and regional setting are well known in the current study area (Andreev et al., 2004, 2009; Ilyashuk et al., 2006; Kienast et al., 2008; Wetterich et al., 2009, 2014). Therefore, the drill sites (Fig. 1c) were chosen to maximize stratigraphic coverage and age with the aim to obtain a permafrost record from the Holocene (MIS 1) back to the Eemian interglacial (MIS 5e; Russian: Kazansevo). Eemian deposits form a paleo-equivalent to the Holocene and are otherwise rather difficult to assess in this area. According to prior studies by Wetterich et al. (2014) and references therein, the cores investigated in this study can be integrated into an already described environmental and climatic history. It has to be mentioned that similar interglacial deposits at Oyogos Yar from the mainland coast opposite to Bol'shoy Lyakhovsky Island have recently been dated. These deposits reveal slightly younger infrared optical stimulated luminescence (IR-OSL, 112.5 ± 9.6 kyr) ages than Eemian (Opel et al., 2017). However, since it is not clear yet, whether both deposits really represent the same age window, we stay here with the interpretation based on the Bol'shoy Lyakhovsky deposits by Andreev et al. (2004).

The field work was conducted in April 2014 as part of the joint Russian-German research project CarboPerm (Schwamborn and Wetterich, 2015). Four cores were drilled using a KMB-3-15M (rotary) drill rig. The drilled core segments were kept frozen and transported in frozen state for further processing to Potsdam, Germany. In our home laboratory sampling was conducted in a climate chamber at -10 °C. 40 inner core samples distributed throughout the cores were taken with exception of intervals where ice-wedges were encountered. Samples were investigated for microbial biomarkers, free (pore-water) and bound acetate concentrations as well as OM characteristics such as total organic carbon (TOC), total organic carbon to total nitrogen (TOC/TN) ratio, hydrogen index (HI) and compositional OM analysis using open-pyrolysis gas chromatography (Pyr-GC).

2.1 Core descriptions

Cores are described stratigraphically from younger to older deposits. Core L14-05 (Fig. 1c) is 7.89 m long and consists of silty fine-grained sediments with scattered organic remains. Overall this core possesses lens-like cryostructures which occur between 1.00 to 2.45 m and 6.71 to 7.89 m core depth. According to prior studies by Andreev et al. (2009) and Wetterich et al. (2009), the upper core section approximately down to 5.5 m consists of a Holocene (MIS 1) unit (Table 1), while the deeper deposits are of MIS 3 age (Russian: Kargin). According to previous paleo-environmental interpretations the MIS 1 deposits represent Alas deposits, where Early Holocene lake sediments have accumulated on top of a MIS 3 surface. During late Holocene time (<3.7 ka BP) the site drained and froze (Andreev et al., 2009).

Core L14-02 (Fig. 1c) is 20.02 m in length. The upper 11.26 m consist of silty fine-grained sediments with macroscopical organic remains and an alternation of horizontal, vertical and reticulated ice veins, and lens-like cryostructures. Below 11.26 m the core consists of an ice wedge, and no samples were taken from this part. The core material is of Late Pleistocene age

(Table 1) and was deposited under subaerial conditions during the last interstadial MIS 3 (Wetterich et al., 2014). The deposits represent the infill of an ice-wedge polygon with a succession of paleosols.

The upper 4.90 m of core L14-03 (15.49 m in length; Fig. 1c) are comparable in their sedimentology and cryostructures to the silty fine-grained sediments of core L14-02. Below 4.90 m the sediment has more sandy portions. The sediments between 4.90 to 8.45 m have visible organic remains and similar cryostructures. Below 8.45 m the sediments are characterized by only scattered organic remains but similar cryostructures as described above. Below 10.90 m the deposits mainly consist of sand and gravel, and in the lowermost 40 cm of gravel. Cryostructures are partly formed as vertically aligned cm-thick ice veins. In earlier studies at the same site these deposits are interpreted to represent MIS 4 (Russian: Zyryan; Table 1) deposits (Andreev et al., 2009).

Core L14-04 (Fig. 1c) is 8.10 m long and consists of silty fine-grained sediments with visible organic remains and cryostructures comparable to core L14-02. Between 4.24 to 4.89 m the core consists of massive ice. The upper 6 m were probably deposited during the MIS 4 stadial period (Table 1). The deposits below 6 m were deposited during the Eemian (MIS 5e; Russian: Kazansevo; Table 1) and appear to represent thermokarst lake sediments (Andreev et al., 2004).

3 Methods

3.1 Organic matter parameters

After freeze-drying and grinding the samples for total organic carbon (TOC) analysis were decalcified with 0.1N HCL. TOC and total nitrogen (TN) (wt%) were determined by a carbon-nitrogen-sulphur elemental analyser (Vario EL III, Elementar) with a device-specific accuracy of ± 0.1 wt%. For further information on characteristic OM parameters the hydrogen index (HI) was determined by Rock-Eval pyrolysis using a Rock-Eval 6 instrument (Behar et al., 2001). Therefore, 17 freeze-dried and ground samples of different TOC content covering all time intervals were analysed. Measurements were conducted by Applied Petroleum Technology AS (Kjeller, Norway). To obtain additional information on the macromolecular structure of the OM, 10 mg from these samples were used for open-system pyrolysis after Horsfield et al. (1989). After the free biomolecules (bitumen) were thermally removed (300 °C), the macromolecular organic matrix was pyrolyzed with temperatures between 300-600 °C. The pyrolysates were trapped (liquid N_2) and finally measured on a pyrolysis-gas chromatograph (AGILENT GC 6890A Chromatograph) equipped with a flame ionization detector (Py-GC-FID). For peak quantification of the detected pyrolysate products *n*-butane was used as external standard. The areas of the detected pyrolysate peaks were integrated and calculated using the AGILENT ChemStation software. For the Eglinton-diagram (Eglinton et al,. 1990) o-xylene, 2,3-dimethylthiophene and *n*-nonene and for the Horsfield-diagram (Horsfield et al., 1989) C_1-C_5 alkane gases, C_6-C_{14}-*n*-alkanes and *n*-alkenes as well as C_{15} and longer *n*-alkanes and *n*-alkenes were integrated. For further details on these methods see Horsfield et al. (1989) and Stapel et al. (2016).

3.2 Low molecular weight organic acids (LMWOAs) analyses

After slow thawing of a subset of the frozen samples at about 4 °C, the pore water within the samples was separated by centrifugation (Sigma, laboratory centrifuge 6K15, 2500 rpm, 20 °C, 10 min). Free LMWOAs such as acetate were measured from pore water samples by ion chromatography with conductivity detection (ICS 3000, Dionex). Furthermore, LMWOAs bound via ester-bonds to the complex OM were analysed by conducting an alkaline ester cleavage approach developed by Glombitza et al. (2009a) on pre-extracted sediment samples. Details are described in Stapel et al. (2016).

3.3 Microbial lipid biomarker analysis

Approximately 30-50 g of the freeze-dried and ground samples were extracted using a flow blending system modified after Bligh and Dyer (1959) as described in Stapel et al. (2016). Subsequently, the obtained sediment extract was separated into four different fractions of increasing polarity (low polar lipids, free fatty acids, glycolipids, and polar lipids) following a method described by Zink and Mangelsdorf (2004). Finally, all four fractions were evaporated to dryness and stored at -20 °C until analysis. After a fatty acid cleavage procedure described in Müller et al. (1998), the phospholipid fatty acids (PLFA) within the polar-lipid fraction were measured by gas chromatography-mass spectrometry (GC-MS). For PLFA quantification an internal standard (1-myristoyl-d27-sn-glycero-3-phosphocholine) was used. PLFAs were identified by means of mass spectrum interpretation and comparison with a standard mixture comprising a series of saturated, unsaturated, branched and cyclo-propyl-fatty acid methyl esters in the range from C_{12} to C_{20}. Details on instrument settings are described in Stapel et al. (2016).

After asphaltene precipitation the low polar-lipid fraction was separated into an aliphatic, aromatic and hetero-compound (containing nitrogen, oxygen and sulphur-components; NSO) fraction using a medium-pressure liquid chromatography system (MPLC) (Radke et al., 1980). An aliquot of the NSO fraction was investigated for tetraether lipids (glycerol dialkyl glycerol tetraether; GDGT) and archaeol using a Shimadzu LC20AD HPLC instrument coupled to a Finnigan TSQ 7000 triple quadrupole MS with an atmospheric pressure chemical ionization (APCI) interface. An external archaeol standard was used for quantification. Details on instrument settings are described in Stapel et al. (2016). The branched vs. isoprenoid tetraether (BIT) index was calculated after Hopmans et al. (2004). The data on individual GDGTs are provided in the supplement (Tables S1 and S2).

3.4 Statistical approaches

For statistical analysis of the measured parameters, the Pearson correlation coefficient (R^2) was computed using the MATLAB R2015b software environment. In addition, p-values were also calculated with the same software and only correlations with $p \leq 0.05$ were evaluated for this study.

4 Results

Characteristic OM parameters (TOC, TOC/TN and HI), biomarkers for living microbial communities (PLFA) and for past bacterial (brGDGTs) as well as archaeal communities (isoGDGT-0 and archaeol) and the concentration of free and bound acetate are presented in figure 2 for all four cores from Bol´shoy Lyakhovsky Island. Every core includes at least one sample (core L14-03 has two samples) representing the overlaying soil as part of the active layer above the permafrost deposits from MIS 1, 3 and 4. Due to the stratigraphic settings at the study site on Bol´shoy Lyakhovsky Island, active layers containing OM from MIS 2 and MIS 5e could not be obtained in the field. Additionally, the results from open-system pyrolysis are shown in figure 3.

4.1 Characteristic OM parameters

Active layers:

In the active layers TOC concentrations are above 2 wt%, except in core L14-05 with 1.5 wt% (Fig. 2a). The TOC/TN ratios range between 8.2 and 11.1 (Fig. 2b). The representative active layer sample for Rock-Eval analysis (L15-05, 10 cm) revealed a HI value of 236 mg HC/g TOC (Fig. 2c). Overall, the samples reveal strongly increased PLFA concentrations (84.1, 149.3, 86.3 and 37.8 µg/g sediment, respectively) compared to the permafrost deposits below (Fig. 2d). The PLFA inventory is composed of saturated FAs ranging from C_{12} to C_{24}, *iso*-branched FAs from C_{13} to C_{19}, *anteiso*-branched FAs from C_{13} to C_{17}, other saturated branched FAs from C_{17} to C_{20}, a saturated mid-chain branched FA 10-Me16:0, a series of mono-unsaturated FAs such as 14:1ω5, 15:1, 16:1ω5*cis/trans* 16:1ω7*cis/trans*, 17:1ω7*cis/trans*, 18:1ω7*cis/trans* and 18:1ω9*cis/trans*, FAs with a cyclopropyl-ring cycl-17:0 and cycl-19:0 as well as some mono-unsaturated branched FAs from C_{15} to C_{17}. The sum of all brGDGT (past bacterial markers) vary between 849.1, and 27.2 ng/g sediment, while concentrations of the isoGDGT-0 with 3.1 to 0.8 ng/g sediment and archaeol (both past archaeal markers) with 17.7 to 2.0 ng/g sediment are much lower in each core (Fig. 2e to 2g). The free acetate concentration (Fig. 2h) is, compared to the rest of the cores, rather low (0.9 to 1.5 mg/l). In contrast, the bound acetate concentrations are comparatively high with 44.5 to 64.2 mg/l (Fig. 2i).

Marine Isotope Stage 1 (MIS 1):

In unit MIS 1 from core L14-05, the TOC, TOC/TN and HI-profiles (Fig. 2a to 2c) all correlate (TOC:TOC/TN, R^2=0.9; p=0.047 and TOC:HI, R^2=0.79; p=0.015). TOC concentrations vary between 1.5 to 1.8 wt%, TOC/TN ratios between 7.1 to 8.2 and HI data between 71 to 194 mg HC/g TOC (H1 to H5; Fig. 2c). Overall, the concentration of PLFAs is lower than in the active layer, ranging between 11 and 27 µg/g sediment (Fig. 2d). Also the diversity of detected FAs decreases with depth. The PLFA profile revealed some similarities to the TOC curve, but no overall correlation was found. Concentrations of past bacterial markers vary between 22.5 and 370.0 ng/g sediment (Fig. 2e). Past archaeal markers vary between 1.0 and 15.0 ng/g sediment for isoGDGT-0 and between 5.4 and 41.1 ng/g sediment for archaeol (Fig. 2f to 2g). The brGDGT profile

correlates well with TOC (R^2=0.9; p=0.015). Free acetate concentrations (Fig. 2h) of about 2.2 mg/l were detected between 0.4 to 2.7 m, followed by an increase to 106 mg/l at 3.3 m depth. Bound acetate concentrations (Fig. 2i) correlate with TOC (R^2= 0.8; p=0.046) and are comparatively low (10.7 mg/l) at 0.4 m depth, but are much higher with concentrations between 29.7 and 48.1 mg/l for the rest of the unit.

Marine Isotope Stage 3 (MIS 3):

Unit MIS 3 comprises the core segments MIS 3-1 of core L14-05 as well as MIS 3-2 and MIS 3-3 of core L14-02 (Table 1, Fig. 2). Overall, TOC and TOC/TN (Fig. 2a, b) correlate (R^2=0.8; p=0.003). The core segment MIS 3-1 shows increased TOC (4.8 wt%) and TOC/TN (12.8) ratios, while core segment MIS 3-2 is characterized by TOC concentrations of 1.4 to 4.7 wt% with a maximum at 1.6 m and TOC/TN ratios between 6.2 to 11.8. Within core segment MIS 3-3, TOC varies from 0.9 to 3.4 wt% and TOC/TN ratios range between 6.2 and 11.9. HI values of 316 (LP1), 322 (LP2) and 126 mg HC/g TOC (LP3) are indicated for unit MIS 3 (Fig. 2c). Figure 2d shows PLFA concentrations of 33 µg/g sediment in core segment MIS 3-1, a decreasing trend from 35.6 to 11.1 µg/g sediment in core segment MIS 3-2, and concentrations between 12.9 to 22.9 µg/g sediment in core segment MIS 3-3. In unit MIS 3 no correlation between PLFA concentrations and TOC is observable. The profile of past bacterial markers (Fig. 2e) in unit MIS 3 generally correlates with TOC (R^2=0.9; p=0.016). Past bacterial and archaeal biomarkers (Fig. 2e to 2g) show higher abundances in the same depth interval, but reach their maximum at a different depth (R^2= 0.8; p=0.021). In MIS 3-1 all past markers are strongly increased (2070.4 ng/g sediment for brGDGTs as well as 133.4 ng/g sediment for isoGDGT-0 and 81.1 ng/g sediment for archaeol). MIS 3-2 is characterized by concentrations between 34.4 and 591.1 ng/g sediment for the brGDGTs as well as between 0.3 and 8.6 ng/g sediment for isoGDGT-0 and 5.9 and 23.2 ng/g sediment for archaeol. Much lower concentrations are observed for MIS 3-3 between 3.7 and 147.7 ng/g sediment for the brGDGTs as well as 0.3 to 1.9 ng/g sediment for isoGDGT-0 and 1 to 10.2 ng/g sediment for archaeol. Free acetate concentrations (Fig. 2h) of 51.1 mg/l are indicated for MIS 3-1, while in MIS 3-2 the free acetate concentrations rise to 412 mg/l at 1.6 m. In MIS 3-3 the highest free acetate concentrations of 757.5 mg/l are measured at 4.2 m depth, followed by decreasing concentrations to 13.8 mg/l and a subsequent rise to 160.0 mg/l. The bound acetate concentrations (Fig. 2i) correlate with TOC (R^2= 0.8; p=0.049) and show a concentration of 59.2 mg/l in MIS 3-1. In the deeper core segments of MIS 3-2 and 3-3 bound acetate concentrations range between 11.7 and 93.7 mg/l with maxima at 1.6 m and 4.2 m depth.

Marine Isotope Stage 4 (MIS 4):

Unit MIS 4 comprises core segments MIS 4-1 of core L14-03 and MIS 4-2 of core L14-04. TOC and TOC/TN ratios (Fig. 2a, b) correlate within unit MIS 4 (R^2=0.8; p=0.009). In core segment MIS 4-1 TOC concentrations range between 2.7 to 1.9 wt% and the TOC/TN ratio between 8.6 and 9.7 in the upper 2.5 m, below TOC concentrations are ≤ 1.5 wt% and TOC/TN ratios are < 6. Core segment MIS 4-2 is characterized by a decreasing TOC trend from 2.4 to 0.5 wt% and TOC/TN ratios from 9 to 4.5. Four HI values were measured in MIS 4-1 with values of 388 (LP4), 226 (LP5), 80 (LP6) and 256 mg HC/ g

TOC (LP7) and one HI value of 276 mg HC/ g TOC (LP8) in MIS 4-2 (Fig. 2c). The PLFA concentrations (Fig. 2d) resemble the TOC contents (R^2= 0.7; p=0.002) with concentrations between 19.4 and 35.5 µg/g sediment in the upper 5 m of MIS 4-1 and lower concentrations of 5.2 to 10.0 µg/g sediment below 6 m. MIS 4-2 shows low PLFA concentrations between 8.1 to 19.2 µg/g sediment. In MIS 4-1 past microbial biomarker profiles (Fig. 2e to 2g) correlate with each other (R^2= 0.8; p=0.031) and with the TOC profile (brGDGTs vs. TOC: R^2=0.7, p=0.047; archaeol vs. TOC: R^2=0.7, P=0.039). The concentrations of bacterial markers generally range between 0.2 and 48.9 ng/g sediment with an increase to 208.0 ng/g sediment at 1.4 m and to 128.0 g/g sediment at 4.7 m depth. For archaeal markers concentrations range generally between 0.4 and 2.8 ng/g sediment for isoGDGT-0 as well as between 0.6 and 38.3 ng/g sediment for archaeol with maxima at 1.4 m and 4.7 m depth. In MIS 4-2 the bacterial GDGT concentrations are decreasing from 294.0 ng/g sediment to 34.2 ng/g sediment and correlate with TOC (R^2=0.9; p=0.018). The archaeal marker concentrations range between 1.0 and 1.5 ng/g sediment for isoGDGT-0 and between 7.0 and 17.4 ng/g sediment for archaeol with a maximum at 5.3 m depth. The isoGDGT-0 and archaeol concentrations do not correlate with the profile of brGDGT markers or with TOC. Within core segment MIS 4-1 free acetate concentrations (Fig. 2h) were below 100.1 mg/l. However, maxima occurred at 2.5 m (193.2 mg/l), and 6.4 m depth (628.5 mg/l). In core segment MIS 4-2 the free acetate concentrations range from 31.2 to 70.0 mg/l. The bound acetate concentrations (Fig. 2i) of unit MIS 4 resemble TOC (R^2=0.7; p=0.018). They are usually characterized by concentrations between 6.7 to 23.7 mg/l with maxima at 3.4 m (61.8 mg/l) and 5.7 m (44.6 mg/l) in MIS 4-1 and decreasing concentrations from 41.7 to 12.1 mg/l in MIS 4-2.

Marine Isotope Stage 5e (MIS 5e):

In unit MIS 5e (Eemian) of core L14-04, TOC and TOC/TN correlate (R^2=0.99; p=0.018) and show TOC contents of about 0.6 wt% and TOC/TN ratios from 3.7 to 4.9 (Fig. 2a, b). Samples from MIS 5e show low HI values (Fig. 2c) of 61 (E1), 81 (E2) and 78 mg HC/gTOC (E3). The PLFA concentrations (Fig. 2d) are between 4.5 to 5.2 µg/g sediment, which is quite low compared to the other intervals and resembles the low TOC profile. All past microbial marker profiles (Fig. 2e to 2g) are low and correlate (R^2=0.9, p=0.036). The concentrations of past bacterial markers vary between 21.7 to 27.1 ng/g sediment, while the concentrations of the archaeal markers range from 1.0 to 1.9 ng/g sediment for isoGDGT-0 and from 2.5 to 3.4 ng/g sediment for archaeol. The free acetate concentration (Fig. 2h) increases from 12.5 to 89.5 mg/l with depth, while the bound acetate concentration (Fig. 2i) scatters between 0.5 to 19.6 mg/l.

4.2 Open system-pyrolysis GC

Results provided by open system-pyrolysis experiments on 17 representative samples (high/low TOC) enable a deeper insight into the OM characteristics. Figure 3a (after Eglinton et al., 1990) classifies the deposited OM into aliphatic-, aromatic- or sulphur-rich OM. All samples from the Holocene (H1, H2, H3, H4, H5) and Eemian (E1, E2, E3) units and two samples from the Late Pleistocene unit (LP3, LP6) fall within the range of OM type III (terrestrial OM Type). Late Pleistocene samples (LP4, LP5, LP7, LP8) corresponding to higher HI values indicate a mixture of OM type III and II

(increased aliphatic character). Two Late Pleistocene sample (LP1, LP2) and the active layer sample (AL), all displaying the highest HI values, fall within the range of OM type II. All samples, especially the samples from the Eemian (MIS 5e), show only a very low abundance of sulphur compounds generated by pyrolysis indicating sulphur lean OM (2,3-dimethylthiophene).

Figure 3b (after Horsfield et al., 1989) suggests different aliphatic characters for the selected samples, indicating an increasing aliphatic character with higher HI and TOC. Samples from the Eemian unit (E1, E2, E3) and the Holocene sample H1 as well as two samples from the Late Pleistocene unit (LP3, LP6) with low HI (< 130) and low TOC (< 1) reveal the weakest aliphatic character. In comparison, the samples from the Holocene unit (H2, H3, H4, H5) with intermediate HI (140-200) and TOC contents > 1 show a slightly increased aliphatic character. All these samples are characterized by OM type III (Fig. 3a). Most of the samples from the Late Pleistocene unit (LP1, LP2, PL4, PL5, PL6, PL7) and the active layer (AL) sample reveal the strongest aliphatic character corresponding to HI > 200 and to TOC >1 and to a mixture of OM type III and II (Fig. 3a, b).

5 Discussion

When permafrost thaws, formerly freeze-locked OM becomes bioavailable again (Wagner et al., 2007; Lee et al., 2012). In order to assess the impact of this OM on future climate evolution, it is of utmost interest to learn more about the degradability of the thawing OM especially with regard to its potential to release greenhouse gases. OM degradability in soils can be influenced by the molecular structure of the source organic material and its decomposition processes during deposition. Thereby, decomposition is affected by environmental factors (temperature, water saturation causing oxic/anoxic conditions and adsorption with the mineral soil matrix) and biological controls concerning the involved microbial ecosystem (Schmidt et al., 2011). In this paper the focus is placed on the organic matter composition and its specific characteristics. However, also environmental and biological controls on OM degradation and accumulation are considered.

5.1 Organic matter characteristics

The composition of permafrost OM is mainly a mix of different terrestrial sources and the result of early diagenetic degradation processes during its deposition in the past (White, 2013). We applied pyrolysis techniques (Rock-Eval pyrolysis and open-system pyrolysis GC-FID) on the OM to get a deeper insight into the structural composition and to define specific characteristics for the OM of different depositional ages.

The highest accumulation of OM up to 4.9% TOC was found in the interstadial deposits of MIS 3 (core sections 3-1 and 3-2), which is in the range also observed in other studies investigating Yedoma deposits (Schirrmeister et al., 2011a; Strauss et al., 2015). The measured TOC/TN ratios of 5 to 12 are within the range of terrestrial permafrost deposits reported for the NE Siberian Arctic (Wetterich et al., 2009; Schirrmeister et al., 2011a; Strauss et al., 2015). Open system-pyrolysis data confirm, as expected, that the permafrost deposits on Bol´shoy Lyakhovsky Island are mainly dominated by terrestrial OM (Type III

OM) (Fig. 3a), although Holocene and Eemian samples are deposited in a thermokarst environment (Wetterich et al., 2009). Pyrolysis experiments of TOC-rich samples from the active layer (core L14-05) and the Late Pleistocene (LP) glacial period (comprising MIS 3 and MIS 4, Table 1) reveal high HI values (Fig. 2c). The Eglinton triangular plot indicates for these samples a Type III OM with a tendency to Type II OM (Fig. 3a). This is mainly caused by a higher aliphatic character of these samples as shown by the Horsfield triangular plot (Fig. 3b). Thus, this TOC-rich OM can be interpreted as terrestrial OM with higher proportions of aliphatic structural moieties. One origin of this aliphatic material could be soil algae OM. Algae are usually rich in aliphatic structural units (Kolattukudy, 1980) and cyanobacteria and green algae are reported for permafrost soils and deposits (Vishnivetskaya, 2009). Thus, these samples might indicate OM accumulation during intervals of increased soil moisture, which would be favourable for algae growth. Periods of increased soil moisture were already reported by Sher et al. (2005) for the LP glacial interval. The LP glacial period (Yedoma deposits) was influenced by climate variations, which resulted in alternating wetter or drier environmental conditions in NE Siberia (Andreev et al., 2009). The generally cool climate and anaerobic soil conditions (due to water saturated soils) during the LP glacial period slowed rates of soil OM decomposition (Dutta et al., 2006) and increased the accumulation of OM (Andreev et al., 2011; Schirrmeister et al., 2011a; Wetterich et al., 2014). The TOC-rich Yedoma deposits (comprising MIS 3 and partly MIS 4) with their higher aliphatic proportion (Figs. 3a and 3b) are indicative for such depositional environments. However, those LP glacial period samples with lower TOC contents and HI values (LP3, LP6; Fig. 2a, c) reveal a minor aliphatic character, which likely reflect a change to a drier depositional environment with less water-saturated soils at the respective time interval.

In contrast, the low TOC concentrations and HI values of the Eemian samples (MIS 5e, Table 1) point to less OM accumulation and/or an increased level of OM decomposition. This could be in line with the warmer and drier climate of the Eemian period in NE Siberia (Andreev et al., 2004; Wetterich et al., 2014; Wetterich et al., 2016), which might have supported intense aerobic microbial degradation of OM due to drier soil conditions (Andreev et al., 2009). The last interglacial was characterized by higher summer temperatures compared to the LP glacial period and even to the Holocene (Bond et al., 2001; Shackleton et al., 2003; Kienast et al., 2008, 2011) and was accompanied by permafrost thawing, draining, thermokarst formation and thermal erosion (Table 2) (Andreev et al., 2009). The open system-pyrolysis data (Fig. 3) indicate for the Eemian deposits (E1, E2, E3) a more pronounced type III OM and a less aliphatic character compared to the Yedoma samples. Comparing the Eemian with the Holocene interglacial deposits (both are interpreted to have comparable vegetation (Kienast et al., 2008)), the Holocene samples are characterized by higher TOC contents, HI values and aliphatic proportions. This might indicate less decomposed OM during deposition and therefore higher favourable characteristics for OM degradation in future than for the Eemian deposits.

In addition to the environmental conditions in our study the OM characteristics might also have been influenced by the depositional settings. Both the Holocene and Eemian OM were deposited in thermokarst lake environments (Wetterich et al., 2009). Comparing the TOC contents from our study with those from thermokarst lakes in the Kolyma region further to the east (Peterse et al., 2014), it becomes clear that the Holocene and Eemian deposits on Bol´shoy Lyakhovsky Island show much lower TOC contents (Holocene 0.21 to 1.81% TOC; Eemian 0.57 to 0.64% TOC) than the Holocene thermokarst

deposits from the Kolyma region (Holocence 4.8 to 22.6% TOC). However, Wetterich et al., (2009) reported that lake deposits in Holocene and Eemian time can vary between lacustrine (around 2 % TOC) and boggy (around 10 to 20 % TOC) characteristics. Thus, the Holocene and Eemian samples in our study seem to reflect lacustrine while those in the study of Peterse et al. (2014) represent boggy conditions. Overall, the thermokast conditions did not lead to higher accumulation of OM in the recovered deposits on Bol´shoy Lyakhovsky Island. In contrast, warmer conditions during the Holocene and Eemian might have caused a higher OM decomposition. This would suggest that for our sample set environmental factors have a stronger impact on the OM accumulation than the depositional characteristics. More investigation on different depositional settings not only with depth and sediment age but also on a regional scale has to be conducted to improve our insights into the role of different depositional settings on the OM characteristics in permafrost regions.

5.2 Signals of present and past microbial communities in permafrost deposits

In order to investigate whether the freeze-locked OM already stimulated a diverse bacterial and archaeal community during deposition in the past, biomarkers for past microbial communities were examined. Especially, intervals with increased abundance of biomarkers characteristic for methanogenic archaea are of interest. This will provide information on to how the deposited OM of different ages already stimulated microbial greenhouse gas production in the past, which will help to assess the potential of the OM for greenhouse gas production upon future permafrost thaw. Since past microbial biomarkers could also be a product of microbial degradation of a presently living microbial community, the Bol´shoy Lyakhovsky samples were also screened with regard to microbial life markers to compare both biomarker records.

As life markers we used phospholipids with ester bound fatty acids (PLFAs), since these bacterial cell membrane components are rapidly degraded after cell death (Logemann et al., 2011). In contrast, intact polar lipids (IPL) with ether bound moieties (diether side chain or tetraethers) have only a restricted potential to act as life markers for bacteria or archaea due to their significantly higher stability (Logemann et al., 2011). Thus, since microbial communities generally consist of both bacteria and archaea, we used the PLFAs here as a general indicator for intervals of increased present microbial life.

The detection of PLFA life markers indicates the occurrence of living bacterial communities in all investigated cores from Bol´shoy Lyakhovsky. While the PLFA signals are low in the permafrost sequences, all active layers contain higher concentrations of PLFAs (Fig. 2d). This indicates a larger microbial community in the surface layers and presumably also increased microbial activity at least during the summer season. According to Knoblauch et al. (2013), permafrost surface layers contain a mix of newly produced and old OM, which can stimulate microbial activity during unfrozen periods. Signals of microbial life in permafrost deposits are strongly decreased compared to the active layer. It has been suggested that the life marker signals in the permafrost section represent most likely living successors of the microbial community incorporated into the sediments during time of deposition (Bischoff et al., 2013). Thus, the permafrost preserved the microbial community of the past. Different studies have shown that the respective microbial cells can be re-activated upon permafrost thaw, after

which they are able to produce greenhouse gases (e.g. Knoblauch et al., 2013; Schuur et al., 2015; Treat et al., 2015; Walz et al., 2017).

Glycerol dialkyl glycerol tetraethers (GDGTs) and archaeol represent past microbial biomass (Stapel et al., 2016). GDGTs and archaeol are the cores of former membrane lipids, which are already partly degraded as indicated by the loss of their head group moieties. However, the core lipids are very stable over geological time scales (Pease et al., 1998; Schouten et al., 2013) and can be found in many different habitats (Bischoff et al., 2013; Schouten et al., 2013). Past bacterial (brGDGTs (Weijers et al., 2006a and 2006b)) and archaeal (isoGDGTs and archaeol (Koga et al., 1993; Pancost et al., 2001)) markers provide information on the abundance of a past microbial community and indirectly might provide information about microbial activity during time of deposition. IsoGDGT-0 (no cyclopentyl-rings in the tetraether alkyl chains) and archaeol are used as markers for methanogenic communities in permafrost and peatland environments (Pancost et al., 2011; Bischoff et al., 2014), whereas their relative proportion varies between different methanogenic genera (Koga and Mori, 2006). PLFA life marker profiles indicate abundant present microbial life only for the active layers and do not correlate with the past biomarkers. Thus, the data suggest that in the permafrost sequence the past markers represent a paleo-signal (Stapel et al., 2016).

The results on past bacterial and archaeal biomarkers (Fig. 2e to 2g) show that intervals with increased concentrations often correspond to increased OM contents (TOC, Fig. 2a) with higher aliphatic character (higher HI values). This can especially be observed in the Yedoma deposits with the core sections MIS 3-1, 3-2 and the upper part of MIS 4-1 and 4-2 (Fig. 2c: LP1, LP2, LP4 and LP8). The archaeol profile (Fig. 2g) suggests the presence of methanogenic communities during these intervals and methane production from this kind of OM in the past. Thus, the microbial past markers indicate that the OM rich Yedoma deposits supported an abundant microbial life including methanogenic archaea during time of deposition. Comparable trends (with some deviations when TOC contents are quite low) can be observed when relating the past biomarkers to gTOC (Fig. S1).

A slight increase in permafrost temperatures is expected to have not only an influence on the soil-moisture content but also on the abundance and diversity of the microbial community (Wagner et al., 2007). Thus, intervals with increased past biomarker concentrations in permafrost regions might reflect increased soil moisture during time of deposition forming favourable living conditions for anaerobic bacteria (Weijers et al., 2006a) and archaea (Wagner et al., 2007). According to Wetterich et al (2014), the MIS 3 interstadial optimum occurred between 48 to 38 ka BP on Bol´shoy Lyakhovsky Island and is characterized by warmer conditions with tundra environments with water-saturated active layers (Meyer et al., 2002; Hubberten et al., 2004; Andreev et al., 2011). This link between warmer and wetter conditions and increased abundance of microbial biomarkers during the interstadial MIS 3 was already observed by Bischoff et al. (2013) on Kurungnakh Island and Stapel et al. (2016) on Buor Khaya peninsula. In their studies comparable or even higher concentrations of brGDGTs, archaeol and isoGDGTs were detected for the Yedoma intervals deposited during warmer and wetter environmental conditions. In contrast, both studies indicated relatively high concentrations of archaeol (up to approximately 80 ng/g sediment and 250 ng/g sediment, respectively) in the active layer sequence, which cannot be observed in the present study.

Methanogenic archaea require anaerobic soil conditions. Thus, the biomarker data suggest lower soil-moisture conditions in the active layers of the drilled cores on Bol´shoy Lyakhovsky Island. An explanation for these lower soil-moisture conditions is that all cores where drilled on high centre polygons, supporting drier surface conditions and with that a deeper penetration of oxygen into the soils.

As outlined above the Holocene (MIS 1) and Eemian (MIS 5e) successions in this study were deposited in a thermokarst lake environment (Andreev et al., 2004, 2009; Wetterich et al., 2009, 2014). Peterse et al. (2014) reported for Holocene surface samples of thermokarst lakes in the Kolyma region much higher concentrations of brGDGTs (ranging between 7037 to 47676 ng/g sediment and 146 to 211 µg/gTOC, respectively) than observed in the current study (20 to 834 ng/gSed and 1.4 to 56 µg/gTOC, Tables S1 and S2). The main reason for this seems to be the different amounts of OM stimulating a larger microbial community in the thermokarst lakes from the Kolyma region.

5.3 Microbial substrate potential for greenhouse gas generation

To assess the potential of the OM from different depositional ages to provide substrates for the production of greenhouse gases, acetate is used as an appropriate substrate for microbial metabolism (Ivarson and Stevenson, 1964; Sørensen and Paul, 1971; Sansone and Martens, 1981; Balba and Nedwell, 1982). Acetate is the terminal electron acceptor for methanogens in cold-temperate environments (Chin and Conrad, 1995; Wagner and Pfeiffer, 1997), especially for acetoclastic methanogens (Thauer, 1998) and methanogenic archaea. Both are ubiquitous in anoxic environments and in permafrost sediments (Kobabe et al., 2004).

In this study two acetate pools are investigated: 1) the free-acetate pool within the pore water, representing an easily and fast accessible substrate source for microbial metabolism and 2) the bound-acetate fraction, which is still linked to the OM. The latter constitutes a future substrate source upon degradation (Glombitza et al., 2009b). Overall, the concentrations of bound acetate (Fig. 2h) in the investigated samples correlate well with the amount of TOC and also often to the HI values. The largest future substrate potential for microbial turnover is associated to MIS 3 (with mean concentrations of ~ 48.9 mg/l), followed by MIS 4 (~ 33.26 mg/l) and MIS 1 (~30.05 mg/l) (Table 2). In contrast, the bound-acetate concentration in the Eemian (MIS 5e) deposits suggests a depleted and possibly already altered bound-substrate pool as the concentration is considerably lower (~ 9.98 mg/l) than in all other deposits.

In the active layer samples the very low concentrations of free acetate together with the elevated concentrations of PLFA life markers suggest a higher microbial consumption of free acetate by an active microbial community (Lee et al., 2012; Knoblauch et al., 2013; Stapel et al., 2016). This activity is most likely stimulated by e.g. warmer temperatures (thawing conditions) and the input of newly produced and old OM during the thawing period. Especially the deepening of the active layer due to global warming increased the accessibility of formerly freeze-locked OM. This old OM was reported to be particularly sensitive to temperature-induced microbial decomposition (Knorr et al., 2005; Davidson and Janssens, 2006) and therefore is considered as an important substrate source for future microbial turnover.

In the present study, the highest PLFA concentration was detected in the active layer of the core sequence containing MIS 3 deposits (core L14-02). This may reflect the high potential of the MIS 3 Yedoma OM to serve as a substrate provider for a living microbial community upon thaw. However, local environmental differences may also affect the PLFA concentration. For example, the core containing MIS 3 deposits was drilled on a stable tundra surface (core L14-02) with relatively stable active layer conditions. In contrast, the other cores were either drilled in a geomorphological dynamic terrace position with thermo-erosion (Schirrmeister et al., 2011; Grosse et al., 2011) and seasonal supply of sediment and water or in a drained and refrozen Holocene thermokarst basin (core L14-05), which is characterized by lower ice contents and shallower active layers (Schwamborn and Wetterich, 2015). Nevertheless, the increased PLFA concentrations in all active layers indicate to a certain extent that the permafrost OM at least from MIS 3, 4 and 1 can serve as good substrate providers in a future permafrost thawing scenario. For MIS 5e OM this could not be evaluated due to the lack of MIS 5e deposits with an active layer on top.

In contrast to the bound acetate concentrations, the free-acetate substrate pool does only partly correlate with the TOC contents in the individual cores (in all cores: $R^2 < 0.5$). The reason for this might be that the free-acetate pool in permafrost pore waters is not only the result of acetate released from the organic source material, but also of other factors influencing the free-acetate signal such as lateral and vertical diffusion promoted by capillary pressure (Parlange, 1971), thawing and freezing processes as well as microbial production and consumption. However, similar trends between acetate (free and bound), TOC and HI are observed at several depth intervals mainly within the MIS 3 and 4 deposits (e.g. core L14-02 at 1.5 and 4.2 m, core L14-03 at 2.5 and 5.8 m, Fig. 2). Here, the mean concentration (~ 93.6 and 82.1 mg/l) of free acetate is at least two to three times higher than that identified in the interglacial periods MIS 1 (46.1 mg/l) or MIS 5e (24.1 mg/l). The smaller free acetate pool in the Holocene deposits may be the result of intense microbial consumption during OM deposition in the past, as has been observed for the modern active layers (see above). This could have been supported by deeper and prolonged thawing of past active layers starting with the onset of the early Holocene, when warming resulted in unstable environmental conditions, especially during the Holocene Optimum (Andreev et al., 2004; Wagner et al., 2007; Wetterich et al., 2008). As a consequence, this could have increased active microbial acetate consumption (Xue et al., 2016). Similarly, the low concentrations of free acetate in the Eemian deposits may also be the result of increased microbial consumption due to warmer environmental conditions. The Eemian is another period associated to intensive permafrost thaw, which again likely altered the free acetate concentration in the sediments due to the lateral transport of water and/or sediment (Andreev et al., 2009). Based on the results obtained in this study it can be noted that sediments from the interglacial periods contain reduced amounts of free acetate in comparison to those from the LP glacial period. Although the free-acetate pool in the Holocene and Eemian deposits is similar low, the Holocene deposits contain at least a considerable bound-acetate future substrate potential (Fig. 2i; Table 2).

Overall the Yedoma deposits (MIS 3 and MIS 4) contain the largest free and bound acetate substrate pools (Fig. 2h, i). They are rich in OM and are characterized by the highest abundance of past microbial biomarkers including those resembling methanogenic communities in wetlands (Fig. 2e to 2g). The Yedoma organic rich material often shows high HI values

assigning an increased aliphatic character to this organic material (Fig. 3a, b). Thus, in contrast to simply using the TOC content, the HI values seem to represent a promising parameter to assess the potential of permafrost OM to act as an appropriate source material for microbial OM degradation. OM with increased HI is considered to contain a higher proportion of better degradable aliphatic molecular structures, whereas OM with a low HI contains a higher proportion of less degradable aromatic structures (Hedges et al., 2000).

Analog results have been obtained for Yedoma deposits in a previous study on Buor Khaya Peninsula about 400 km SW from Bol'shoy Lyakhovsky Island (Stapel et al., 2016). Considering the thickness of the LP Yedoma deposits on Bol'shoy Lyakhovsky Island (20 m, Schennen et al., 2016) and across Siberia (10-60 m, Dutta et al., 2006) as well as the extension of these deposits across Russia (about 1 028 264 km^2, Grosse et al., 2013), it becomes obvious that the freeze-locked Yedoma deposits represent a significant substrate potential for future microbial greenhouse gas generation. Ongoing warming in the Arctic will increase the depth range of the active layer making deeper and older OM bioavailable for microbial decomposition.

6 Conclusions

The potential of OM in terms of providing organic substrates for microbial induced greenhouse gas production varies within the investigated permafrost deposits from the Eemian to the present time and is mainly controlled by environmental and climatic conditions. The strongest present and future substrate potential appears to be stored within the Yedoma OM deposits from the last interstadial (MIS 3) and stadial (MIS 4) period, which is characterized by increased HI values and a higher aliphatic character. Thus, this currently frozen Yedoma OM is likely to have a strong impact on the greenhouse gas driven climate-carbon feedback cycle upon thaw. In contrast, the interglacial periods (Holocene and especially Eemian) show lower substrate potentials, which might point to stronger microbial degradation during time of deposition. The Eemian deposits reveal both low present and future substrate pools. However, the Holocene deposits at least contain a significant future-substrate pool, which may become available when recycled in the active layer.

Data availability

https://www.pangaea.de/ (follows after acceptance and includes all shown datasets)

Author contributions

J. G. Stapel conducted sub-sampling of the core material, the laboratory analyses and data interpretations guided by K. Mangelsdorf and B. Horsfield. G. Schwarmborn and L. Schirrmeister planned and coordinated the fieldwork as well as drilled and processed the core material. J. G. Stapel wrote the manuscript commented by all co-authors.

Competing interests

The authors declare that they have no conflict of interest.

Acknowledgments

This research was supported by the German Ministry of Education and Research as part of the bilateral CarboPerm Project between Germany and Russia (grant no. 03G0836B). We thank all Russian and German participants of the drilling expedition, especially Mikhail N. Grigoriev (Melnikov Permafrost Institute, Yakutsk, Russia) for his leadership. We thank the three reviewers for their thoughtful and very constructive comments and suggestions on our manuscript.

References

Andreev, A. A., Grosse, G., Schirrmeister, L., Kuzmina, S. A., Novenko, E. Y., Bobrov, A. A., Tarasov, P. E., Ilyashuk, B. P., Kuznetsova, T. V., Brbetschek, M., Meyer, H. and Kunitsky, V.V.: Late Saalian and Eemian palaeoenvironmental history of the Bol´shoy;shoy Lyakhovsky Island (Laptev Sea region, Arctic Siberia), Boreas, 33(4), 319-348, doi: 10.1111/j.1502-3885.2004.tb01244.x, 2004.

Andreev, A. A., Grosse, G., Schirrmeister, L., Kuznetsova, T. V., Kuzmina, S. A , Bobrov, A. A., Tarasov, P. E., Novenko, E. Y., Meyer, H., Derevyagin, A. Y., Kienast, F., Bryantseva, A. and Kunitsky, V. V.: Weichselian and Holocene palaeoenvironmental history of the Bol´shoy Lyakhovsky Island, New Siberian Archipelago, Arctic Siberia, Boreas, 38(1), 72-110, doi: 10.1111/j.1502-3885.2008.00039.x, 2009.

Andreev, A. A., Schirrmeister, L., Tarasov, P. E., Ganopolski, A., Brovkin, V., Siegert, C., Wetterich, S. and Hubberten, H.-W.: Vegetation and climate history in the Laptev Sea region (Arctic Siberia) during Late Quaternary inferred from pollen records, Quaternary Science Reviews, 30(17), 2182-2199, doi: 10.1016/j.quascirev.2010.12.026, 2011.

Anisimov, O. A.: Potential feedback of thawing permafrost to the global climate system through methane emission, Environmental Research Letters, 2(4), 045016, doi:10.1088/1748-9326/2/4/045016, 2007.

Arkhangelov, A., Mikhalev, D. and Nikolaev, V.: Reconstruction of formation conditions of permafrost and climates in Northern Eurasia, History of Permafrost Regions and Periglacial Zones of Northern Eurasia and Conditions of Old Human Settlement"(AA Velichko, AA Arkhangelov, OK Borisova, et al., Eds.), 85-109, 1996.

Balba, M. T. and Nedwell, D. B.: Microbial metabolism of acetate, propionate and butyrate in anoxic sediment from Colne Point Saltmarsch, Essex, U.K., Journal of General Microbiology, 128(7), 1415-1422, doi: 10.1099/00221287-128-7-1415, 1982.

Beer, C.: Soil science: The Arctic carbon count, Nature Geoscience, 1(9), 569-570, doi: 10.1038/ngeo292, 2008.

Behar, F., Beaumont, V. and Penteado, H. D. B.: Rock-Eval 6 technology: performances and developments, Oil & Gas Science and Technology, 56(2), 111-134, doi:10.2516/ogst:2001013, 2001.

Bischoff, J., Mangelsdorf, K., Gattinger, A., Schloter, M., Kurchatova, A. N., Herzschuh, U. and Wagner, D.: Response of methanogenic archaea to Late Pleistocene and Holocene climate changes in the Siberian Arctic, Global Biogeochemical Cycles, 27(2), 305-317, doi: 10.1029/2011GB004238, 2013.

Bischoff, J., Mangelsdorf, K., Schwamborn, G. and Wagner, D.: Impact of Lake-Level and Climate Changes on Microbial Communities in a Terrestrial Permafrost Sequence of the El'gygytgyn Crater, Far East Russian Arctic, Permafrost and Periglacial Processes, 25(2), 107-116, doi: 10.1002/ppp.1807, 2014.

Bligh, E. G. and Dyer, W. J.: A rapid method of total lipid extraction and purification, Canadian journal of biochemistry and physiology, 37(8), 911-917, doi: 10.1139/o59-099, 1959.

Bond, G., Kromer, B., Beer, J., Muscheler, R., Evans, M. N., Showers, W., Hoffmann, S., Lotti-Bond, R., Hajdas, I. and Bonani, G.: Persistent solar influence on North Atlantic climate during the Holocene, Science, 294(5549), 2130-2136, doi: 10.1126/science.1065680, 2001.

Carter, M. R. and Gregorich, E. G.: Soil sampling and methods of analysis, Taylor and Francis, London, 1224 p, 2008.

Chapin III, F. S., Sturm, M., Serreze, C. M., McFadden, J. P., Key, J. R., Lloyd, A. H., McGuire, A. D., Rupp, T. S., Lynch, A. H., Schimel, J. P., Beringer, J., Chapman, W. L., Epstein, H. E., Euskirchen, E. S., Hinzman, L. D., Jia, G., Ping, C. L.,

Tape, K. D., Thompson, C. D. C., Walker, A. D. and Welker, J. M.: Role of Land-Surface Changes in Arctic Summer Warming, Science, 310(5748), 657-660, doi: 10.1126/science.1117368, 2005.

Chin, K.-J. and Conrad, R.: Intermediary metabolism in methanogenic paddy soil and the influence of temperature, FEMS microbiology ecology, 18(2), 85-102, doi: 10.1111/j.1574-6941.1995.tb00166.x, 1995.

Dahl-Jensen, D., Albert, M., Aldahan, A., Azuma, N., Balslev-Clausen, D., Baumgartner, M., Berggren, A.-M., Bigler, M., Binder, T. and Blunier, T.: Eemian interglacial reconstructed from a Greenland folded ice core, NATURE, 493(7433), 489-494, doi: 10.1038/nature11789, 2013.

Davidson, E. A. and Janssens, I. A.: Temperature sensitivity of soil carbon decomposition and feedbacks to climate change, NATURE, 440(7081), 165-73, doi: 10.1038/nature04514, 2006.

Dutta, K., Schuur, E. A. G., Neff, J. C. and Zimov, S. A.: Potential carbon release from permafrost soils of Northeastern Siberia, Global Change Biology, 12(12), 2336-2351, 2006.

Eglinton, T. I., Sinninghe Damsté, J. S., Kohnen, M. E. and de Leeuw, J. W.: Rapid estimation of the organic sulphur content of kerogens, coals and asphaltenes by pyrolysis-gas chromatography, Fuel, 69(11), 1394-1404, doi: 10.1016/0016-2361(90)90121-6, 1990.

Flanagan, L. B. and Syed, K. H.: Stimulation of both photosynthesis and respiration in response to warmer and drier conditions in a boreal peatland ecosystem, Global Change Biology, 17(7), 2271-2287, doi: 10.1111/j.1365-2486.2010.02378.x, 2011.

Fontaine, S., Barot, S., Barre, P., Bdioui, N., Mary, B. and Rumpel, C.: Stability of organic carbon in deep soil layers controlled by fresh carbon supply, NATURE, 450(7167), 277-280, doi: 10.1038/nature06275, 2007.

French, H. M.: The periglacial environment 3rd ed., John Wiley & Sons, Ltd, England, 2007.

Glombitza, C., Mangelsdorf, K. and Horsfield, B.: Maturation related changes in the distribution of ester bound fatty acids and alcohols in a coal series from the New Zealand Coal Band covering diagenetic to catagenetic coalification levels, Organic Geochemistry, 40(10), 1063-1073, doi: 10.1016/j.orggeochem.2009.07.008, 2009a.

Glombitza, C., Mangelsdorf, K. and Horsfield, B.: A novel procedure to detect low molecular weight compounds released by alkaline ester cleavage from low maturity coals to assess its feedstock potential for deep microbial life, Organic Geochemistry, 40(2), 175-183, doi: 10.1016/j.orggeochem.2008.11.003, 2009b.

Grosse, G., Schirrmeister, L., Siegert, C., Kunitsky, V. V., Slagoda, E. A., Andreev, A. A. and Dereviagyn, A. Y.: Geological and geomorphological evolution of a sedimentary periglacial landscape in Northeast Siberia during the Late Quaternary, Geomorphology, 86(1-2), 25-51, doi: 10.1016/j.geomorph.2006.08.005, 2007.

Grosse, G., Romanovsky, V., Jorgenson, T., Anthony, K. W., Brown, J., Overduin, P. P. and Wegener, A.: Vulnerability and feedbacks of permafrost to climate change, EOS, Transactions American Geophysical Union, 92, 73-74, doi: 10.1029/2011eo090001, 2011.

Grosse, G., Robinson, J. E., Bryant, R., Taylor, M. D., Harper, W., DeMasi, A., Kyker-Snowman, E., Veremeeva, A., Schirrmeister, L. and Harden, J.: Digital database of the distribution of late Pleistocene ice-rich syngenetic permafrost of the Yedoma Suite in East and Central Siberia, Russia, U.S. Geological Survey Open-File Report, 1-37 (1078), 2013.

Haack, S. K., Garchow, H., Odelson, D. A., Forney, L. J. and Klug, M J.: Accuracy, Reproducibility, and Interpretation of Fatty Acid Methyl Ester Profiles of Model Bacterial Communities, Applied and Environmental Microbiology, 60(7), 2483-2493, 1994.

Hedges, J. I., Eglinton, G., Hatcher, P. G., Kirchman, D. L., Arnosti, C., Derenne, S., Evershed, R. P., Kögel-Knabner, I., de Leeuw, J. W., Littke, R., Michaelis, W. and Rullkötter, J.: The molecularly-uncharacterized component of nonliving organic matter in natural environments, Organic Geochemistry, 31(10), 945-958, doi: 10.1016/S0146-6380(00)00096-6, 2000.

Hopmans, E.C., Weijers, J.W.H., Schefuss, E., Herfort, L., Sinninghe Damsté, J.S., Schouten, S.: A novel proxy for terrestrial organic matter in sediments based on branched and isoprenoid tetraether lipids, Earth and Planetary Science Letters 24, 107–116, doi: 10.1016/j.epsl.2004.05.012, 2004.

Horsfield, B., Disko, U. and Leistner, F.: The micro-scale simulation of maturation: outline of a new technique and its potential applications, Geologische Rundschau, 78(1), 361-373, doi: 10.1007/BF01988370, 1989.

Hubberten, H. W., Andreev, A. A., Astakhov, V. I., Demidov, I., Dowdeswell, J. A., Henriksen, M., Hjort, C., Houmark-Nielsen, M., Jakobsson, M., Kuzmina, S., Larsen, E., Lunkka, J. P., Lysa, A., Mangerud, J., Möller, P., Saarnistov, M., Schirrmeister, L., Sher, A. V., Siegert, C., Siegert, M. J. and Svendsen, J. I.: The periglacial climate and environment in

northern Eurasia during the Last Glaciation, Quaternary Science Reviews, 23(11-13), 1333-1357, doi: 10.1016/j.quascirev.2003.12.012, 2004.

Hugelius, G., Strauss, J. Zubrzycki, S., Harden, J. W., Schuur, E. A. G., Ping, C. L., Schirrmeister, L., Grosse, G., Michaelson, G. J., Koven, C. D., O´Donnell, J. A., Elberling, B., Mishra, U., Camill, P., Yu, Z., Palmtag, J. and Kuhry, P.: Estimated stocks of circumpolar permafrost carbon with quantified uncertainty ranges and identified data gaps, Biogeosciences, 11(23), 6573-6593, doi: 10.5194/bg-11-6573-2014, 2014.

Ilyashuk, B. P., Andreev, A. A., Bobrov, A. A., Tumskoy, V. E. and Ilyashuk, E. A.: Interglacial History of a Palaeo-lake and Regional Environment: A Multi-proxy Study of a Permafrost Deposit from Bol'shoy Lyakhovsky Island, Arctic Siberia, Journal of Paleolimnology, 35(4), 855-872, doi: 10.1007/s10933-005-5859-6, 2006.

Ivanov, O.: Stratigrafiya i korrelatsiya Neogenykh i Chetvertichnykh otlozheniyakh subarkticheskikh ravnin Vostochnoi Yakutii (Stratigraphy and correlation of Neogene and Quaternary deposits of subarctic plains in Eastern Yakutia), Problemy izucheniya Chetvertichnogo perioda (Problems of the Quaternary Studies). InNauka, Moscow, 202-211, 1972.

Ivarson, K. and Stevenson, I.: The decomposition of radioactive acetate in soils: II. The distribution of radioactivity in soil organic fractions, Canadian journal of microbiology, 10(5), 677-682, doi: 10.1139/m64-087, 1964.

Kienast, F., Tarasov, P., Schirrmeister, L., Grosse, G. and Andreev, A. A.: Continental climate in the East Siberian Arctic during the last interglacial: Implications from palaeobotanical records, Global and Planetary Change, 60(3-4), 535-562, doi: 10.1016/j.gloplacha.2007.07.004, 2008.

Kienast, F., Wetterich, S., Kuzmina, S., Schirrmeister, L., Andrev, A., Tarasov, P., Nazarova, L., Kossler, A., Frolova, A., Kunitsky, V. V.: Paleontological records indicate the occurrence of open woodlands in a dry inland climate at the present-day Arctic coast in western Beringia during the last interglacial, Quaternary Science Reviews, 30, 2134-2159, doi:10.1016/j.quascirev.2010.11.024, 2011.

Knoblauch, C., Beer, C., Sosnin, A., Wagner, D. and Pfeiffer, E.-M.: Predicting long-term carbon mineralization and trace gas production from thawing permafrost of Northeast Siberia, Glob Chang Biol, 19(4), 1160-1172, doi: 10.1111/gcb.12116, 2013.

Knorr, W., Prentice, I. C., House, J. I. and Holland, E A.: Long-term sensitivity of soil carbon turnover to warming, NATURE, 433(7023), 298-301, doi: 10.1038/nature03226, 2005.

Kobabe, S., Wagner, D. and Pfeiffer, E.-M.: Characterisation of microbial community composition of a Siberian tundra soil by fluorescence in situ hybridisation, FEMS microbiology ecology, 50(1), 13-23, doi: 10.1016/j.femsec.2004.05.003, 2004.

Koga, Y., Nishihara, M., Morii, H. and Akagawa-Matshushita, M.: Ether Polar Lipids of Methanogenic Bacteria: Structures, Comparative Aspects, and Biosyntheses, Microbiological Reviews, 57(1), 164-182, 1993.

Koga, Y. and Morii, H.: Special methods for the analysis of ether lipid structure and metabolism in archaea, Analytical biochemistry, 348(1), 1-14, 20096.

Kolattukudy, P. E.: Biopolyester membranes of plants: cutin and suberin, Science, 208(4447), 990-1000, 1980.

Koven, C. D., Ringeval, B., Friedlingstein, P., Ciais, P., Cadule, P., Khvorostyanov, D. V., Krinner, G. and Tarnocai, C.: Permafrost carbon-climate feedbacks accelerate global warming, Proceedings of the National Academy of Sciences, 108(36), 14769-14774, doi: 10.1073/pnas.1103910108, 2011.

Kuhry, P., Ping, C. L., Schuur, E. A., Tarnocai, C. and Zimov, S.: Report from the International Permafrost Association: carbon pools in permafrost regions, Permafrost and Periglacial Processes, 20(2), 229-234, doi: 10.1002/ppp.648, 2009.

Lawrence, D. M. and Slater, A. G.: A projection of severe near-surface permafrost degradation during the 21st century, Geophysical Research Letters, 32(4), doi: 10.1029/2005GL025080, 2005.

Lee, H., Schuur, E. A. G., Inglett, K. S., Lavoie, M. and Chanton, J. P.: The rate of permafrost carbon release under aerobic and anaerobic conditions and its potential effects on climate, Global Change Biology, 18(2), 515-527: doi: 10.1111/j.1365-2486.2011.02519.x, 2012.

Liljedahl, A. K., Boike, J., Daanen, R. P., Fedorov, A. N., Frost, G. V., Grosse, G., Hinzman, L. D., Iijma, Y., Jorgenson, J. C., Matveyeva, N., Necsoiu, M., Raynolds, M. K., Romanovsky, V. E., Schulla, J., Tape, K. D., Walker, D. A., Wilson, C. J., Yabuki, H. and Zona, D.: Pan-Arctic ice-wedge degradation in warming permafrost and its influence on tundra hydrology, Nature Geoscience, 9, p. 312-318, doi:10.1038/ngeo2674, 2016.

Lipson, D. A., Zona, D., Raab, T. K., Bozzolo, F., Mauritz, M. and Oechel, W. C.: Water-table height and microtopography control biogeochemical cycling in an Arctic coastal tundra ecosystem, Biogeosciences, 9, 577-591, doi: 10.5194/bgd-8-6345-2011, 2012.

Logemann, J., Graue, J., Köster, J., Engelen, B., Rullkötter, J. and Cypionka, H.: A laboratory experiment of intact polar lipid degradation in sandy sediments: Biogeosciences, v. 8(9), p. 2547-2560, doi:10.5194/bg-8-2547-2011, 2011.

McGuire, A. D., Anderson, L. G., Christensen, T. R., Dallimore, S., Guo, L., Hayes, D. J., Heimann, M., Lorenson, T. D., Macdonald, R. W. and Roulet, N.: Sensitivity of the carbon cycle in the Arctic to climate change, Ecological Monographs, 97(4), 523-555, doi: 10.1890/08-2025.1, 2009.

Meyer, H., Dereviagin, A., Siegert, C., Schirrmeister, L. and Hubberten, H.-W.: Palaeoclimate reconstruction on Big Lyakhovsky Island, north Siberia - hydrogen and oxygen isotopes in ice wedges, Permafrost and Periglacial Processes, 13(2), 91-105, doi: 10.1002/ppp.416, 2002.

Meyers, P. A. and Teranes, J. L.: Sediment organic matter, Tracking environmental change using lake sediments, Springer, p. 239-269, 2002.

Mu, C., Zhang, T., Schuster, P. F., Schaefer, K., Wickland, K. P., Repert, A. D., Liu, L., Schaefer, T. and Cheng, G.: Carbon and geochemical properties of cryosols on the North Slope of Alaska, Cold Regions Science and Technology, 100, 59-67, doi: 10.1016/j.coldregions.2014.01.001, 2014.

Mueller, C. W., Rethemeyer, J., Kao-Kniffin, J., Loppmann, S., Hinkel, K. M. and Bockheim, G.: Large amounts of labile organic carbon in permafrost soils of northern Alaska, Glob Chang Biol., 21(7), 2804-2817, doi: 10.1111/gcb.12876, 2015.

Müller, K. D., Schmid, E. N. and Kroppenstedt, R. M.: Improved identification of mycobateria by using the microbial identification system in combination with additional trimethylsulfonium hydroxide pyrolysis, Journal of Clinical Microbiology, 36(9), 2477-2480, 1998.

Opel T. Wetterich S., Meyer H., Dereviagin A. Yu., Fuchs M. C. and Schirrmeister L.: Ground-ice stable isotopes and cryostratigraphy reflect late Quaternary palaeoclimate in the Northeast Siberian Arctic (Oyogos Yar coast, Dmitry Laptev Strait), Clim. Past, 13, 587–611, doi.org/10.5194/cp-13-587-2017, 2017.

Pancost, R. D., Hopmans, E. C. and Sinninghe Damste, J. S.: Archaeal lipids in Mediterranean cold seeps: molecular proxies for anaerobic methane oxidation, Geochimica et Cosmochimica Acta, 65(10), 1611-1627, doi: 10.1016/S0016-7037(00)00562-7, 2001.

Pancost, R. D., McClymont, E. L., Bingham, E. M., Roberts, Z., Charman, D. J., Hornibrook, E. R. C., Blundell, A., Chambers, F. M., Lim, K. L. H. and Evershed, R. P.: Archaeol as a methanogen biomarker in ombrotrophic bogs, Organic Geochemistry, 42(10), 1279-1287; doi: 10.1016/j.orggeochem.2011.07.003, 2011.

Parlange, J.-Y.: Theory of water-movement in soils: I. one-demensional absorption, Soil science, v. 111(2), 134-137, 1971.

Pease, T. K., Van Vleet, E. S., Barre, J. S. and Dickins, H. D.: Simulated degradation of glyceryl ethers by hydrous and flash pyrolysis, Organic Geochemistry, 29(4), 979-988, doi: 10.1016/S0146-6380(98)00047-3, 1998.

Peterse, F., Vonk, J. E., Holmes, R. M., Giosan, L., Zimov, N. and Eglinton, T. I.: Branched glycerol dialkyl glycerol tetraethers in Arctic lake sediments: Source and implications for paleothermometry at high latitudes, JGR Biogeosciences, 119, 1738-1754, doi:10.1002/2014JG002639, 2014.

Radke, M., Willsch, H. and Welte, D. H.: Preparative hydrocarbon group type determination by automated medium pressure liquid chromatography, Anal. Chem., 52(3), 406-411, doi:10.1021/ac50053a009, 1980.

Romanovsky, V. E., Drozdov, D. S., Oberman, N. G., Malkova, G. V., Kholodov, A. L., Marchenko, S. S., Moskalenko, N. G., Sergeev, D. O., Ukraintseva, N. G., Abramov, A. A., Gilichinsky, D. A. and Vasiliev, A. A.: Thermal state of permafrost in Russia, Permafrost and Periglacial Processes, 21(2), 136-155, doi:10.1002/ppp.683, 2010.

Sansone, F. J. and Martens, C. S.: Methane production from acetate and associated methane fluxes from anoxic coastal sediments, Science, 211(4483), 707-709, doi:10.1126/science.211.4483.707, 1981.

Schadel, C., Schuur, E. A. G., Bracho, R., Elberling, B., Knoblauch, C., Lee, H., Luo, Y., Shaver, G. R. and Turetsky, M. R.: Circumpolar assessment of permafrost C quality and its vulnerability over time using long-term incubation data, Glob Chang Biol, 20(2), 641-52, doi: 10.1111/gcb.12417, 2014.

Schennen, S., Tronicke, J., Wetterich, S., Allroggen, N., Schwamborn, G. and Schirrmeister, L.: 3D ground-penetrating radar imaging of ice complex deposits in northern East Siberia, Geophysics, 81(1), WA195-WA202, doi: 10.1190/geo2015-0129.1, 2016

Schimel, J. and Schaeffer, S.: Microbial control over carbon cycling in soil. Front. Microbiol., 3(348), 155- 165, doi: 10.3389/fmicb.2012.00348., 2012.

Schirrmeister, L., Siegert, C., Kuznetsova, T. V., Kuzmina, S. A., Andreev, A. A., Kienast, F., Meyer, H. and Bobrov, A. A.: Paleoenvironmental and paleoclimatic records from permafrost deposits in the Arctic region of Northern Siberia, Quaternary International, 89(1), 97-118, doi: 10.1016/S1040-6182(01)00083-0, 2002.

Schirrmeister, L., Grosse, G., Wetterich, S., Overduin, P. P., Strauss, J., Schuur, E. A. G. and Hubberten, H.-W.: Fossil organic matter characteristics in permafrost deposits of the northeast Siberian Arctic, Journal of Geophysical Research, 116, doi: 10.1029/2011JG001647, 2011a.

Schirrmeister, L., Kunitsky, V., Grosse, G., Wetterich, S., Meyer, H., Schwamborn, G., Babiy, O., Derevyagin, A. and Siegert, C.: Sedimentary characteristics and origin of the Late Pleistocene Ice Complex on north-east Siberian Arctic coastal lowlands and islands – A review, Quaternary International, 241(1-2), 3-25, doi: 10.1016/j.quaint.2010.04.00, 2011b.

Schirrmeister, L., Froese, D., Tumskoy, V., Grosse, G. and Wetterich, S.: Yedoma: Late Pleistocene Ice-Rich Syngenetic Permafrost of Beringia, In: Elias S.A. (ed.) the Encyclopedia of Quaternary Science, 3, 542-552, doi: 10.1016/B978-0-444-53643-3.00106-0, 2013.

Schmidt, M. W., Torn, M. S., Abiven, S., Dittmar, T., Guggenberger, G., Janssens, I. A., Kleber, M., Kogel-Knabner, I., Lehmann, J., Manning, D. A., Nannipieri, P., Rasse, D. P., Weiner, S. and Trumbore, S. E.: Persistence of soil organic matter as an ecosystem property, NATURE, 478(7367), 49-56, doi: 10.1038/nature10386, 2011.

Schouten, S., Hopmans, E. C. and Sinninghe Damsté, J. S.: The organic geochemistry of glycerol dialkyl glycerol tetraether lipids: A review, Organic Geochemistry, 54, 19-61, doi:10.1016/j.orggeochem.2012.09.006, 2013.

Schuur, E. A., Bockheim, J., Canadell, J. G., Euskirchen, E., Field, C. B., Goryachkin, S. V., Hagemann, S., Kuhry, P., Lafleur, P. M., Lee, H., Mazhitova, G., Nelson, F. G., Rinke, A., Romanovsky, V. E., Shiklomanov, N., Tarnocai, C., Venevsky, S., Vogel, J. G. and Zimov, S. A.: Vulnerability of Permafrost Carbon to climate Change: Implications for the Global Carbon Cycle, Biogeosciences, 58, 701-714, doi: 10.1641/B580807, 2008.

Schuur, E. A., McGuire, A. D., Schädel, C., Grosse, G., Harden, W. J., Hayes, D. J., Hugelius, G., Koven, C. D., Kuhry, P., Lawrence, D. M., Natali, S. M., Olefeldt, D., Romanovsky, V. E., Schaefer, K., Turetsky, M. R., Treat, C. C. and Vonk, J. E.: Climate change and the permafrost carbon feedback, NATURE, 520(7546), 171-179, doi: 10.1038/nature14338, 2015.

Schwamborn, G. and Wetterich, S.: Russian-German Cooperation CARBOPERM: Field campaigns to Bol´shoy Lyakhovsky Island in 2014, Berichte zur Polar-und Meeresforschung, Alfred Wegener Insitute for Polar and Marine Research, Germany, 2015, doi:10.2312/BzPM_0686_2015

Shackleton, N. J., Sánchez-Goñi, M. F., Pailler, D. and Lancelot, Y.: Marine Isotope Substage 5e and the Eemian Interglacial, Global and Planetary Change, 36(3), 151-155, doi: 10.1016/S0921-8181(02)00181-9, 2003.

Sher, A. V., Kuzmina, S. A., Kuznetsova, T. V. and Sulerzhitsky, L. D.: New insights into the Weichselian environment and climate of the East Siberian Arctic, derived from fossil insects, plants, and mammals, Quaternary Science Reviews, 24(5), 533-569, doi: 10.1016/j.quascirev.2004.09.007, 2005.

Sørensen, L. H. and Paul, E.: Transformation of acetate carbon into carbohydrate and amino acid metabolites during decomposition in soil, Soil Biology and Biochemistry, 3(3), 173-180, doi:10.1016/0038-0717(71)90012-5, 1971.

Stapel, J. G., Schirrmeister, L., Overduin, P. P., Wetterich, S., Strauss, J., Horsfield, B. and Mangelsdorf, K.: Microbial lipid signatures and substrate potential of organic matter in permafrost deposits: Implications for future greenhouse gas production, Journal of Geophysical Research: Biogeosciences, 121(10), 2652-2666, doi: 10.1002/2016JG003483, 2016.

Strauss, J., Schirrmeister, L., Mangelsdorf, K., Eichhorn, L., Wetterich, S. and Herzschuh, U.: Organic-matter quality of deep permafrost carbon – a study from Arctic Siberia, Biogeosciences, 12(7), 2227-2245, doi:10.5194/bg-12-2227-2015, 2015.

Talbot, M. R., and Livingstone, D. A.: Hydrogen index and carbon isotopes of lacustrine organic matter as lake level indicators, Palaeogeography, Palaeoclimatology, Palaeoecology, 70, 121-137, doi:10.1016/0031-0182(89)90084-9, 1989.

Thauer, R. K.: Biochemistry of methanogenesis: atribute to Marjory Stephenson, Microbiology, 144(9), 2377-2406, 1998.

Treat, C. C., Natali, S. M., Ernakovich, J., Iversen, C. M., Lupascu, M., McGuire, A. D., Norby, R. J., Roy Chowdhury, T., Richter, A., Santruckova, H., Schadel, C., Schuur, E. A., Sloan, V. L., Turetsky, M. R. and Waldrop, M. P.: A pan-Arctic synthesis of CH4 and CO2 production from anoxic soil incubations, Global Change Biology, 21(7), 2787-2803, doi: 10.1111/gcb.12875, 2015.

Vishnivetskaya T.A.: Viable Cyanobacteria and Green Algae from the Permafrost Darkness. In: Margesin R. (eds) Permafrost Soils. Soil Biology, Vol 16. Springer, Berlin, Heidelberg, 2009.

Vonk, J. E., Tank, S. E., Bowden, W. B., Laurion, I., Vincent, W. F., Alekseychik, P., Amyot, M., Billet, M., Canario, J. and Cory, R. M.: Reviews and syntheses: Effects of permafrost thaw on Arctic aquatic ecosystems, Biogeosciences, 12(23), 7129-7167, doi: 10.5194/bg-12-7129-2015, 2015.

Wagner, D. and Pfeiffer, E.-M.: Two temperature optima of methane production in a typical soil of the Elbe river marshland, FEMS microbiology ecology, 22(2), 145-153, doi: 10.1111/j.1574-6941.1997.tb00366.x, 1997.

Wagner, D., Wille, C., Kobabe, S. and Pfeiffer, E.-M.: Simulation of freezing-thawing cycles in a permafrost microcosm for assessing microbial methane production under extreme conditions, Permafrost and Periglacial Processes, 14(4), 367-374, doi: 10.1002/ppp.468, 2003.

Wagner, D., Gattinger, A., Embacher, A., Pfeiffer, E.-M., Schloter, M. and Lipski, A.: Methanogenic activity and biomass in Holocene permafrost deposits of the Lena Delta, Siberian Arctic and its implication for the global methane budget, Global Change Biology, 13(5), 1089-1099, doi: 10.1111/j.1365-2486.2007.01331.x, 2007.

Waldrop, M. P., Wickland, K. P., White III, R., Berhe, A. A., Harden, J. W. and Romanovsky, V. E.: Molecular investigations into a globally important carbon pool: Permafrost-protected carbon in Alaskan soils, Global Change Biology, 16(9), 2543-2554, doi: 10.1111/j.1365-2486.2009.02141.x, 2010.

Walz, J., Knoblauch, C., Böhme, L. and Pfeiffer, E. M.: Regulation of soil organic matter decomposition in permafrost-affected Siberian tundra soils - Impact of oxygen availability, freezing and thawing, temperature, and labile organic matter, Soil biology and biochemistry, doi: 10.1016/j.soilbio.2017.03.001, 2017.

Washburn, A. L.: Permafrost Features as Evidence of Climatic Change Earth-Science Reviews, 15, 327-402, doi: 10.1016/0012-8252(80)90114-2, 1980.

Weijers, J. W., Schouten, S., Hopmans, E. C., Geenevasen, J. A., David, O. R., Coleman, J. M., Pancost, R. D. and Sinninghe Damste, J. S.: Membrane lipids of mesophilic anaerobic bacteria thriving in peats have typical archaeal traits, Environmental microbiology, 8(4), 648-657, doi: 10.1111/j.1462-2920.2005.00941.x, 2006a.

Weijers, J.W.H., Schouten, S., Spaargaren, O.C., Sinninghe Damsté, J.S.: Occurrence and distribution of tetraether membrane lipids in soils: Implications for the use of the TEX86 proxy and the BIT index. Organic Geochemistry 37, 1680–1693, 2006b.

Wetterich, S., Kuzmina, S., Andreev, A. A., Kienast, F., Meyer, H., Schirrmeister, L., Kuznetsova, T. and Sierralta, M.: Palaeoenvironmental dynamics inferred from late Quaternary permafrost deposits on Kurungnakh Island, Lena Delta, Northeast Siberia, Russia: Quaternary Science Reviews, 27(15), 1523-1540, doi: 10.1016/j.quascirev.2008.04.007, 2008.

Wetterich, S., Schirrmeister, L., Andreev, A. A., Pudenz, M., Plessen, B., Meyer, H. and Kunitsky, V. V.: Eemian and Late Glacial/Holocene palaeoenvironmental records from permafrost sequences at the Dmitry Laptev Strait (NE Siberia, Russia), Palaeogeography, Palaeoclimatology, Palaeoecology, 279(1-2), 73-95, doi: 10.1016/j.palaeo.2009.05.002, 2009.

Wetterich, S., Rudaya, N., Tumskoy, V., Andreev, A. A., Opel, T., Schirrmeister, L. and Meyer, H.: Last Glacial Maximum records in permafrost of the East Siberian Arctic, Quaternary Science Reviews, 30(21-22), 3139-3151, doi: 10.1016/j.quascirev.2011.07.020, 2011.

Wetterich, S., Tumskoy, V., Rudaya, N., Andreev, A. A., Opel, T., Meyer, H., Schirrmeister, L. and Hüls, M.: Ice Complex formation in arctic East Siberia during the MIS3 Interstadial, Quaternary Science Reviews, 84, 39-55, doi: 10.1016/j.quascirev.2013.11.009, 2014.

Wetterich, S., Tumskoy, V., Rudaya, N., Kuznetsov, V., Maksimov, F., Opel, T., Meyer, H., Andreev, A. A. and Schirrmeister, L.: Ice Complex permafrost of MIS5 age in the Dmitry Laptev Strait coastal region (East Siberian Arctic), Quaternary Science Reviews, 147, 298-311, doi: 10.1016/j.quascirev.2015.11.016, 2016.

White, D. C., Davis, W. M., Nickels, J. S., King, J. D. and Bobbie, R. J.: Determination of the sedimentary microbial biomass by extractible lipid phosphate Oecologia, 40(1), 51-62, doi: 10.1007/BF00388810, 1979.

White, R. E.: Principles and practice of soil science: the soil as a natural resource, John Wiley & Sons, 2013.

Xue, K., Yuan, M. M., Shi, Z. J., Qin, Y., Deng, Y., Cheng, L., Liyou, W., He, Z., Van Nostrand, J. D., Bracho, R., Natali, S., Schuur, E. A., Luo, C., Konstantinidis, K. T., Wang, Q., Cole, C. R., Tiedje, J., Luo, Y. and Zhou, J.: Tundra soil carbon is vulnerable to rapid microbial decomposition under climate warming, Nature Climate Change, 6(6), 595-600, doi: 10.1038/nclimate2940, 2016.

Zelles, L.: Fatty acid patterns of phospholipids and lipopolysaccharides in the characterisation of microbial communities in soil: a review, Biol Fertil Soils, 29, 111-129, doi: 10.1007/s003740050533, 1999.

Zimov, S. A., Davydov, S. P., Zimova, G. M., Davydova, A. I., Schuur, E. A. G., Dutta, K. and Chapin III, F. S.: Permafrost carbon: Stock and decomposability of a globally significant carbon pool, Geophysical Research Letters, 33(20), L20502, doi: 10.1029/2006GL027484, 2006.

Zimov, N., Zimov, S., Zimova, A., Zimova, G., Chuprynin, V. and Chapin III, F. S.: Carbon storage in permafrost and soils of the mammoth tundra-steppe biome: Role in the global carbon budget, Geophysical Research Letters, 36(2), doi: 10.1029/2008GL036332, 2009.

Zink, K. G. and Mangelsdorf, K.: Efficient and rapid method for extraction of intact phospholipids from sediments combined with molecular structure elucidation using LC-ESI-MS-MS analysis, Analytical and bioanalytical chemistry, 380(5-6), 798-812, doi:10.1007/s00216-004-2828-2, 2004.

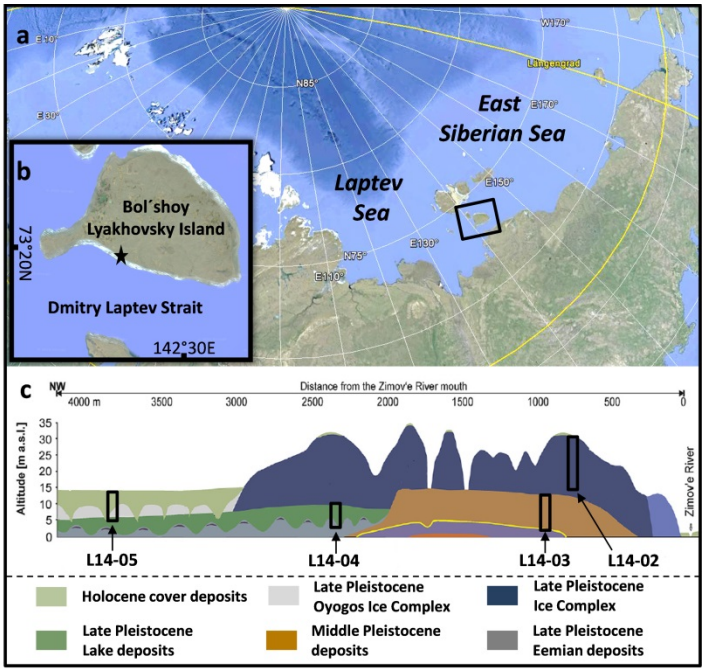

Figure 1: a) Position of Bol´shoy Lyakhovsky Island in the Siberian Arctic. b) Study site on Bol´shoy Lyakhovsky Island indicated by a black star and c) location of the drilled cores comprising different age intervals (L14-05, L14-02, L14-03 and L14-04) modified after Wetterich et al. (2009, 2014) and Schwamborn and Wetterich (2015).

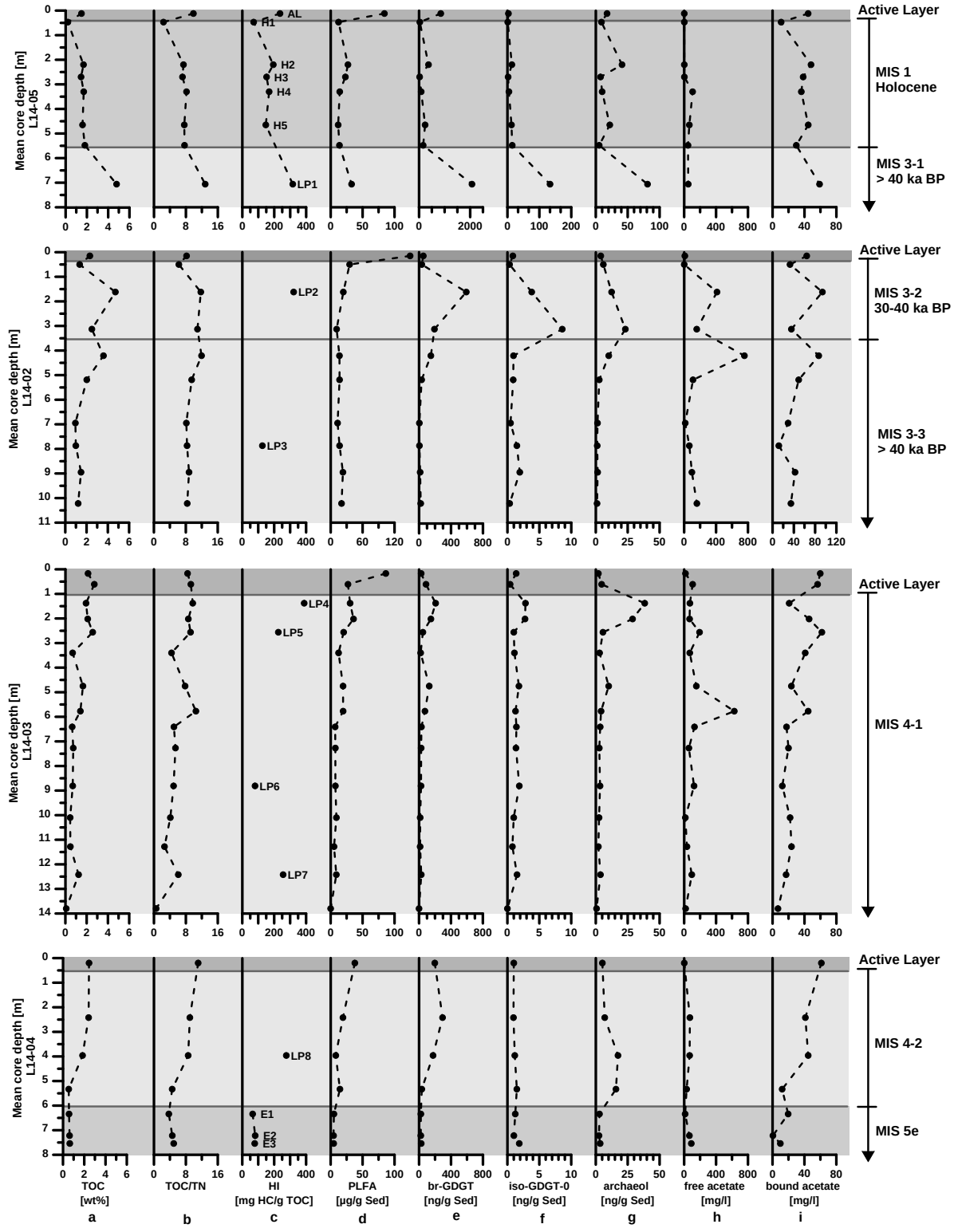
Mean core depth [m]
L14-05
AL
H1
H2
H3
H4
H5
LP1
Active Layer
MIS 1
Holocene
MIS 3-1
> 40 ka BP
Mean core depth [m]
L14-02
LP2
LP3
Active Layer
MIS 3-2
30-40 ka BP
MIS 3-3
> 40 ka BP
Mean core depth [m]
L14-03
LP4
LP5
LP6
LP7
Active Layer
MIS 4-1
Mean core depth [m]
L14-04
LP8
E1
E2
E3
Active Layer
MIS 4-2
MIS 5e
TOC
[wt%]
a
TOC/TN
b
HI
[mg HC/g TOC]
c
PLFA
[µg/g Sed]
d
br-GDGT
[ng/g Sed]
e
iso-GDGT-0
[ng/g Sed]
f
archaeol
[ng/g Sed]
g
free acetate
[mg/l]
h
bound acetate
[mg/l]
i

Figure 2: Bio- and geochemical parameters of permafrost cores L14-05, L14-02, L14-03 and L14-04 from Bol´shoy Lyakhovsky Island, northern Siberia, presented with respect to core depth (left axis) as well as stratigraphic and age units (right column). The vertical profiles show (note partly different x-axis): a) the total organic carbon (TOC) content in wt%, b) the ratio of TOC and total nitrogen (TN), c) the hydrogen index (HI) in mg HC/g TOC, d) the concentration of phospholipid fatty acids (PLFAs) in µg/g sediment, e) the concentration of branched glycerol dialkyl glycerol tetraethers (brGDGTs), f) of isoGDGT-0 and g) of archaeol all in ng/g sediment, h) the concentration of free acetate and i) of bound acetate both in mg/l. Active layer samples are dyed in dark grey, interglacial periods (MIS 1 and MIS 5e) in grey and the last glacial period (MIS 3 and MIS 4) in light grey. According to age, stratigraphy and core segments, the MIS 3 unit is subdivided into the core segments MIS 3-1, 3-2 as well as 3-3 and the MIS 4 unit into the segments MIS 4-1 and 4-2. Sample labels within the HI profile correspond to core samples of different ages (H: Holocene; LP: Late Pleistocene glacial period; E: Eemian).

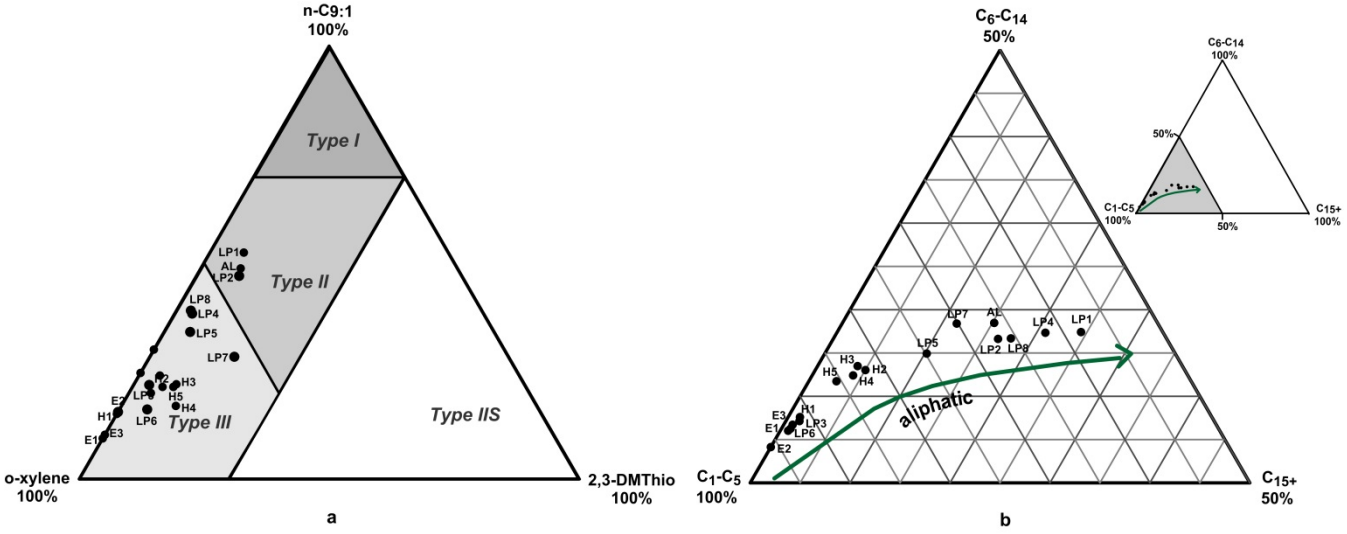

Figure 3: Triangular plots derived from organic matter (OM) open-system pyrolysis. (a) Eglinton-diagram: Classification of the kerogen type (type I/II: aquatic and marine; type III: terrestrial; type IIS: enriched sulphur content) due to the relative abundance of 1,2 dimethylbenzene (ortho-xylene), *n*-nonene (*n*-C9:1) and 2,3-dimethylthiophene (2,3DMThio) in the OM after Eglinton et al. (1990). (b) Horsfield-diagram: Composition of the OM according to the chain length distribution of short (C_1-C_5), intermediate (C_6-C_{14}) and long chain (C_{15+}) *n*-alkanes and *n*-alk-1-enes after Horsfield et al. (1989). The arrow indicates an increasing aliphatic proportion in the OM of the investigated samples. Sample labels correspond to core samples of different ages (H: Holocene; LP: Late Pleistocene glacial period; E: Eemian) with different total organic carbon (TOC) and hydrogen index (HI) values (Fig. 2a and 2c).

Table 1: Schematic overview on the age assignment of the core material drilled on Bol'shoy Lyakhovsky Island showing the different cores with their drilling positions in relation to different age periods (interval names, marine isotope stages (MIS) and Russian terminology (RT) for the respective time periods). The age assignment is based on information obtained from Andreev et al. (2004, 2009) and Wetterich et al. (2004, 2009, 2014).

Cores	Drill Site	Age		
		Period	MIS	RT
L14-05	73.34994°N 141.24156°E	Holocene (interglacial)	1	Holocene
L14-02	73.33623°N 141.32761°E	Late Pleistocene Glacial Period (glacial) interstadial	3	Kargin
L14-03	73.33464°N 141.32822°E	stadial	4	Zyryan
L14-04	73.34100°N 141.28587°E	Eemian (interglacial)	5e	Kazansevo

975

Table 2: Schematic summary compiling the age assignment (time period and marine isotope stage (MIS) classification) of the core material from Bol'shoy Lyakhovsky Island based on Andreev et al. (2004, 2009) and Wetterich et al. (2004, 2009, 2014), the paleoenvironmental information on the different time intervals ([1]Schirrmeister et al., 2002, [2]Andreev et al., 2009, [3]Grosse et al., 2007, [4]Sher et al., 2005, [5]Schirrmeister et al., 2011a, [6]Wetterich et al., 2014), the core sections and the assessment of the organic matter (OM) from different ages to act as a substrate provider for microbial greenhouse gas production (present (free acetate) and future (bound acetate) substrate potential). The substrate potential was classified into very good (++), good (+) and poor (-) based on the results of the current study.

980

Age		Paleoenvironment	Core sections		Substrate potential	
Period	MIS				present	future
Holocene (interglacial)	1	- climate warming[1], permafrost thawing[2] - moisture increase, thermokarst formation[2] - unstable environmental conditions[2] - dissected landscape influenced by local hydrology[3]	L14-05	1	-	+
Late Pleistocene Glacial Period (glacial) interstadial	3	- increased temperature and soil moisture[4] - high organic matter accumulation[5] - optimum: warm and dry (48 to 38 ka BP)[6] - warmer summers, open vegetation[2]		3-1	-	+ +
			L14-02	3-2	+ +	+ +
				3-3	+	+
stadial	4	- cold and dry climate[6] - harsh climate conditions[2] - thin snow cover, low precipitation[2]	L14-03	4-1	+	+
			L14-04	4-2	-	+
Eemian (interglacial)	5e	- warmer climate, open-grass tundra similar to today[2] - permafrost thawing[2] - optimum: 4-5 °C higher summer temperatures than today, shrub tundra[2]		5e	-	-

985